Available online at www.sciencedirect.com
ScienceDirect
Journal of Photochemistry and Photobiology A: Chemistry 194 (2008) 92–96
Journal of Photochemistry and Photobiology A:Chemistry
www.elsevier.com/locate/jphotochem

J-type aggregation of a simple merocyanine skeleton: Spectral features and structure of 4-amino-6-oxopyrimidine

Kenta Goto [a,*], Rieko Omae [a], Minoru Yamaji [b], Teruo Shinmyozu [a]

[a] *Institute for Materials and Chemistry and Engineering (IMCE) and Department of Molecular Chemistry, Graduate School of Sciences, Kyushu University, 6-10-1 Hakozaki, Higashi-ku, Fukuoka 812-8581, Japan*
[b] *Department of Chemistry, Gunma University, Tenjin-cyo, 1-5-1 Kiryu, Gunma 376-8515, Japan*

Received 28 December 2006; received in revised form 10 July 2007; accepted 25 July 2007
Available online 31 July 2007

Abstract

The absorption and fluorescence spectral properties of 4-amino-6-oxopyrimidine (**1**), which has a simple streptopolymethine merocyanine skeleton, clearly showed that the molecule **1** formed the aggregate $\mathbf{1}_n$, and showed an exciton band, appearing at an absorption of 350 nm due to the red-shifted HOMO–LUMO transition. Upon light irradiation of the exciton band, a fluorescence band at 398 nm ($\Phi_{FL} = 0.10$) was observed, and its decay lifetimes were determined. Based on these spectral features, the aggregated $\mathbf{1}_n$ was found to be formed by J-type aggregation. The molecular orientation **1** in the crystal was revealed as being both parallel π–π stacking and hydrogen bonding chains.

Keywords: Exciton interaction; J-aggregate; Merocyanine; Fluorescence; Self-assembly

1. Introduction

Highly organized dye aggregates with particular optical and photophysical properties have important consequences in nature, such as photosynthetic light-harvesting systems [1–3], basic materials [4–6], and in optical materials [7–9]. In particular, an exciton interaction among dye aggregates caused by electronic coupling among the constituent molecules plays an important role in their photophysical properties, and is currently the focus of wide attention, given the connection of their electronic properties to nanoscale structured systems [10]. The well-known merocyanines are this class of dyes having an exciton interaction in solution and crystalline states [11], in mesoporous films [12], in the aggregated dimer [13,14], and in the supramolecular aggregates [15]. On the other hand, for a simple streptopolymethine merocyanine, there seem to be no experimental efforts aiming at a general understanding of the excitonic nature of its aggregates.

A simple streptopolymethine merocyanine is composed of electron donating nitrogen and electron accepting oxygen, linked by a conjugated odd number of methine carbons. In terms of resonance theory, their π-electronic structure lies between those of the neutral and charge-separated forms (Scheme 1a). Due to the asymmetrical contribution of the two forms, merocyanines are peculiar in their optical and photophysical properties, such as pronounced solvatochromism [16,17], photo-isomerism [18], and large hyperpolarizabilities [19,20]. Although theoretical studies of a streptopolymethine merocyanine predict that exciton interaction is present among its aggregates [21], very little experimental evidence has been reported so far.

Motivated by the attractive potential of the simple streptopolymethine merocyanine [22–24], we initiated optical studies of the excitonic properties of self-associated 4-amino-6-oxopyrimidine (**1**) as a basic constituent molecule (Scheme 1b) for the following reasons. First, the simple streptopolymethine merocyanine moiety is included in the molecular structure of **1**. The fixed w-like merocyanine skeleton in molecule **1** would eliminate the chemical instability and the thermal isomerism [25] as observed in the streptopolymethine merocyanine. Second, since molecule **1** has several hydrogen bonding sites, self-association of **1** forms an ordered aggregated structure.

In this paper, we report the aggregated $\mathbf{1}_n$ has an exciton interaction by forming a J-type aggregate. Molecule **1** in concentrated solution was found to emit fluorescence upon excitation of the

* Corresponding author. Tel.: +81 92 642 2723; fax: +81 92 642 2735.
E-mail address: g2k@ms.ifoc.kyushu-u.ac.jp (K. Goto).

1010-6030/$ – see front matter © 2007 Elsevier B.V. All rights reserved.
doi:10.1016/j.jphotochem.2007.07.019

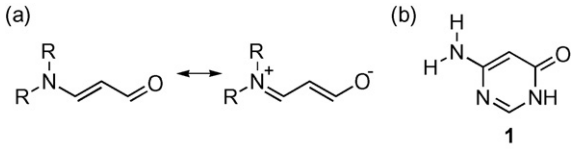

Scheme 1. (a) Neutral and charge-separated forms of streptopolymethine merocyanine. (b) Molecular structure of 4-amino-6-oxopyrimidine (**1**).

exciton band, as well as in the crystalline state. The optical properties related to the molecular orientations of the aggregate $\mathbf{1}_n$ are reported.

2. Experimental

2.1. Materials and reagents

4-Amino-6-oxopyrimidine (**1**) was prepared according to the literature [22–24]. The purity of the compound **1** was checked by means of HPLC, and estimated as 99.9% or higher. Ethanol (fluorometry grade) was purchased from Kanto Chemical, and distilled from CaH_2 prior to each measurement. Anthracene was purchased from Wako Pure Chemical Industries Ltd., as a standard grade, and was used without further purification.

2.2. Measurements

The UV absorption spectra of **1** were recorded on a Jasco V-550 double-beam spectrometer. Fluorescence spectra of **1** in solution and solid states were recorded on a Jasco F-750 and F-4500, respectively. The fluorescence quantum yields were determined by using anthracene ($\Phi = 0.3$) as the standard [26]. The emission lifetime was determined by the single-photon counting method with an FL-900 CDT spectrophotometer (Edinburgh Analytical Instruments, UK).

2.3. Crystal structure of *1*

2.3.1. X-ray diffraction data collections and structure determination

Single crystals of **1** suitable for X-ray diffraction studies were obtained by recrystallization from ethanol. The X-ray data were collected on a Rigaku RAXIS-RAPID Imaging Plate diffractometer with graphite monochromated Mo Kα radiation ($\lambda = 0.71069$ Å). The structure determination was performed using the direct method technique with SIR 97 and a full-matrix least squares refinement based on F^2. All-non-hydrogen atoms were refined anisotropically, while the hydrogen atoms were identified from the difference Fourier map and isotropically refined (CCDC 631240).

2.3.2. Crystal data

$C_4H_5ON_3$, $M = 111.10$, monoclinic, $P2_1/n$ (no. 14), $a = 4.7647(3)$ Å, $b = 11.457(1)$ Å, $c = 8.7032(7)$ Å, $\beta = 96.756(4)^\circ$, $U = 471.80(6)$ Å^3, $Z = 4$, $T = 113$ K, $D_c = 1.564$ g cm^{-3}, μ (Mo Kα) = 1.19 cm^{-1}, $2\theta_{max} = 55.0^\circ$, 4030 reflections were collected, of which 1073 were unique, 93 parameters, GOF = 1.50, $R_1 = 0.035$ ($I > 2(\sigma)I$), $wR_2 = 0.097$ ($I > 2(\sigma)I$), residual electron density: 0.34 and −0.25 eÅ^{-3}.

3. Results and discussion

The UV absorption spectra of **1** at various concentrations in ethanol are shown in Fig. 1. In a dilute solution of **1**, the absorption maximum appeared at 256 nm with a shoulder around 273 nm. The absorption spectrum tails off at 343 nm. These spectral features did not change in the concentration range of 0.19–6.5 × 10^{-4} M. However, by increasing the concentration of **1** above 1.3 × 10^{-3} M, the absorption spectra significantly changed. The optical density of the absorption maximum at 256 nm decreased by 2.5% with increasing concentration. In addition, a new absorption band at 360 nm appears with increasing concentration. These absorption spectra changes apparently originated from the self-association of **1**. We have observed aggregated species in the ethanolic solution of **1**, such as dimer ($[2M + Na]^+ = 245.04$), trimer ($[3M + Na]^+ = 356.07$), and tetramer ($[4M + Na]^+ = 467.10$) by ESI-mass spectrum (Fig. 1S). As generally known for molecules such as polynucleotide DNA, the dipole–dipole interactions between chromophoric bases in the preferred molecular orientations lead to a hypochromic shift as a function of the distance and the direction of the transition moments [27]. Therefore, the former hypochromic shift can be attributed to the presence of a parallel arrangement of transition dipole in the aggregate $\mathbf{1}_n$. Since molecule **1** has electron donating nitrogen and accepting oxygen, the electrostatic interactions in the aggregated $\mathbf{1}_n$ would also affect other transitions. To consider the corresponding new absorption band, we carried out theoretical calculations, and measured the absorption spectra in various solvents.

State energies of the excited states of the monomer **1** were calculated by the INDO/S CI method with the use of the B3LYP/6-31+G(d,p) optimized ground state structure. The theoretical calculations show that the electronic structure of the lowest-lying singlet excited state (3.96 eV) is of an essentially forbidden $^1(n\pi^*)$, and that of the next excited state (4.34 eV) is of a strongly allowed $^1(\pi\pi^*)$ having a HOMO-LUMO transition (Table 1S and Fig. 2S). These results provide evidence

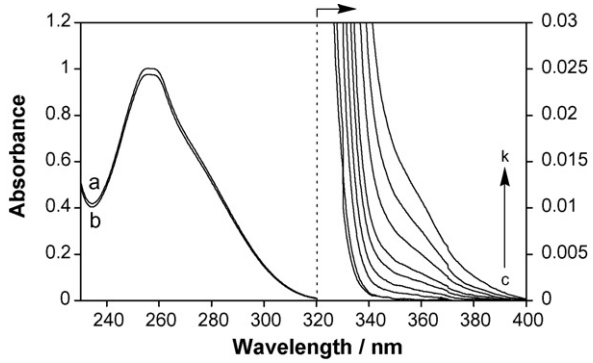

Fig. 1. Absorption spectra of **1** at different concentrations in ethanol: (a) 0.16 mM (optical path length; 10 mm), (b) 3.2 mM (optical path length; 0.5 mm), (c) 0.48 mM, (d) 0.65 mM, (e) 1.3 mM, (f) 1.9 mM, (g) 2.9 mM, (h) 4.8 mM, (i) 6.5 mM, (j) 9.6 mM, and (k) 13.0 mM (optical path length; 50 mm).

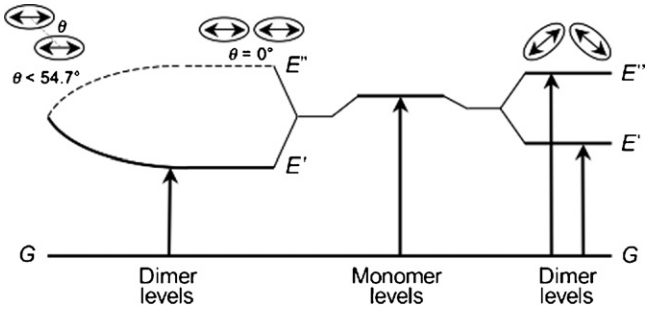

Scheme 2. Exciton splitting of the electronic excited states for a molecular dimer. Coplanar transition dipoles inclined to an interconnected axis by an angle $\theta < 54.7^\circ$ (left), in line transition dipoles (middle), and oblique transition dipoles (right). The double head arrows represent the polarization axis for the molecular electronic transition considered.

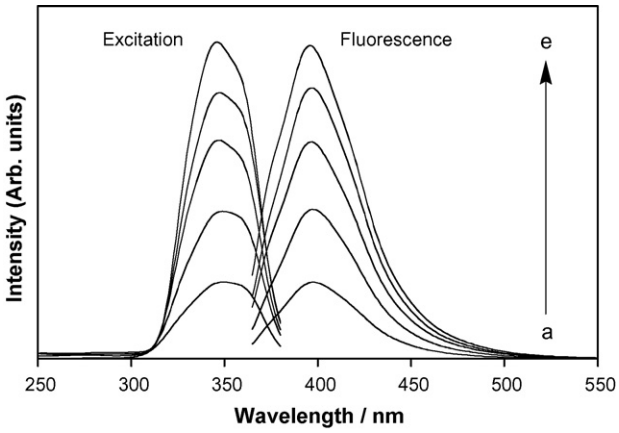

Fig. 2. Excitation and fluorescence spectra of **1** at various concentrations in ethanol: (a) 3.1 mM, (b) 6.2 mM, (c) 9.9 mM, (d) 12.3 mM, and (e) 15.4 mM. The excitation and monitored wavelengths were 350 nm and 400 nm, respectively.

that the absorption maximum is located at 276 nm, corresponding to the HOMO–LUMO transition in the dioxane solution of **1**. This band appeared at 272 nm in acetonitrile solution (Fig. 3S and Table 2S). Upon changing the solvent composition from dioxane to water, the band responsible for the HOMO–LUMO transition shifted toward shorter wavelengths with an increase of the absorption intensity (Fig. 4S). The observed spectral features of **1** account for a negative solvatochromism [28]. Namely, by increasing the solvent polarity, the band for the HOMO–LUMO transition was accompanied by a shift to shorter wavelength. The solvatochromic properties of **1** are consistent with theoretical predictions that the dipole moment of the ground state (S_0: 4.8 D) is more polar than that of the excited state (S_2: 2.1 D) (Table 1S). Therefore, the HOMO–LUMO transition for molecule **1** is found to be sensitive to the surrounding polarity, namely, electrostatic interactions. With the aggregated $\mathbf{1}_n$, the corresponding new band is considered to be due to a red-shifted HOMO–LUMO transition.

We have observed that the absorption band in the shorter wavelengths undergoes hypochromic shift, and that a new absorption band appears in high concentrations of **1**. These observations could be explained by the molecular exciton model [29]. A schematic energy diagram limited to the red-shifted dimer cases is illustrated in Scheme 2. According to exciton theory [29], the dipole–dipole interactions in the dimers predicts a splitting of the excited states. The energy levels of exciton bands of the dimer depend on the geometry of the monomer unit in the aggregate. Coplanar-displacement dimers with interconnected axes by an angle of $\theta < 54.7^\circ$ (left), linear head-to-tail dimers (middle), and oblique head-to-tails dimers (right), all of them called J-type dimers or J-aggregates [4,6,30], show a red-shift transition. They are also characterized by emission bands.

In the diluted ethanol solution of **1**, fluorescence could not be detected. Despite the fact that the temperature was maintained at 77 K, the monomeric **1** did not show any indication of fluorescence. The characteristic excitation and fluorescence spectra of the aggregate $\mathbf{1}_n$ were obtained as shown in Fig. 2. Upon excitation of the absorption band for the aggregated $\mathbf{1}_n$ at 350 nm, the fluorescence band was located around 398 nm. The fluorescence band grew with increasing concentration in the range of $3.1–20 \times 10^{-3}$ M. The excitation spectra monitored at 400 nm appeared as a rather broad band around 351 nm with a shoulder at 356 nm. The relationship between the excitation and the fluorescence spectra is not a clear mirror-image. Additionally, it should be noted that the excitation spectra of the aggregated $\mathbf{1}_n$ significantly differs from the absorption spectra of the monomeric **1**, but corresponded to the absorption band for the aggregated $\mathbf{1}_n$. The fluorescence originated from the lowered absorption band among dye aggregates, coinciding with the typical characteristics for a J-aggregate [4,30]. Therefore, the observed absorption band in the aggregated $\mathbf{1}_n$ is attributed to exciton bands of the J-type aggregate.

To obtain additional insights about the fluorescence from the aggregated $\mathbf{1}_n$, we measured the fluorescence spectra as a function of the excitation wavelength at several concentrations. The obtained results are summarized in Table 1

Table 1
The selected excitation and fluorescence spectral data of **1** at several concentrations in ethanol as a function of the fluorescence wavelength and the excitation wavelength[a]

Excitation wavelength (nm)	3.3×10^{-3} M		2.0×10^{-2} M		Fluorescence wavelength (nm)	3.3×10^{-3} M		2.0×10^{-2} M	
	λ_{FL} (nm)	$\Delta\upsilon_{FL}$[b] (cm^{-1})	λ_{FL} (nm)	$\Delta\upsilon_{FL}$[b] (cm^{-1})		λ_{EX} (nm)	$\Delta\upsilon_{EX}$[b] (cm^{-1})	λ_{EX} (nm)	$\Delta\upsilon_{EX}$[b] (cm^{-1})
340	398	3181	397	3289	395	354	4064	350	3542
345	399	3090	397	3238	400	356	3998	351	3550
350	399	3047	398	3181	420	–[c]	–[c]	351	3565

[a] Full details of data see: Fig. 5S and Table 3S.
[b] FWHM: the full-width at half maximum of the peak.
[c] Not determined.

(Fig. 5S and Table 3S). It was found that the fluorescence and the excitation spectra depend on the wavelength of the irradiating light. By changing the excitation wavelength from 340 nm to 350 nm, the peak maximum of the fluorescence band slightly shifted to longer wavelengths with decreasing peak width. These spectral features were similar to those of the fluorescence bands for both low and high concentrations. On the other hand, when we fixed the light monitored at 400 nm, the peak maximum of the excitation spectra appeared at around 356 nm for a concentration of 3.3 mM ethanol in **1**. For the higher concentration, the peak maximum of the excitation was located at 351 nm.

The present results on the differences of the excitation bands between low and high concentrations indicate two possibilities. First, the aggregated $\mathbf{1}_n$ formed solely a J-type aggregate with several vibronic structure at the given concentration. Next, the presence of several J-type aggregates among the self-assembled **1** is considered. To decide which of the two explanations is more plausible, we measured the fluorescence lifetime in the aggregated $\mathbf{1}_n$.

The fluorescence intensity linearly increased with increasing concentration. On the other hand, the fluorescence quantum yield lies nearly at 0.10 in the range of 0.1 to 2×10^{-2} M (Fig. 6S). The fluorescence decay profiles in the concentrated ethanol solution of **1** are shown in Fig. 3. The fluorescence was found to decay with two components. The fluorescence decay lifetimes and its amplitude are summarized in Table 2. In 1.5×10^{-2} M ethanolic solution of **1**, a short component has a decay lifetime of 2.1 ns (27%), and the following component has 4.8 ns (73%). With increasing the concentration to 2.0×10^{-2} M, the fluorescence decay lifetime and the amplitude of a short component were 2.9 ns and 50%, respectively.

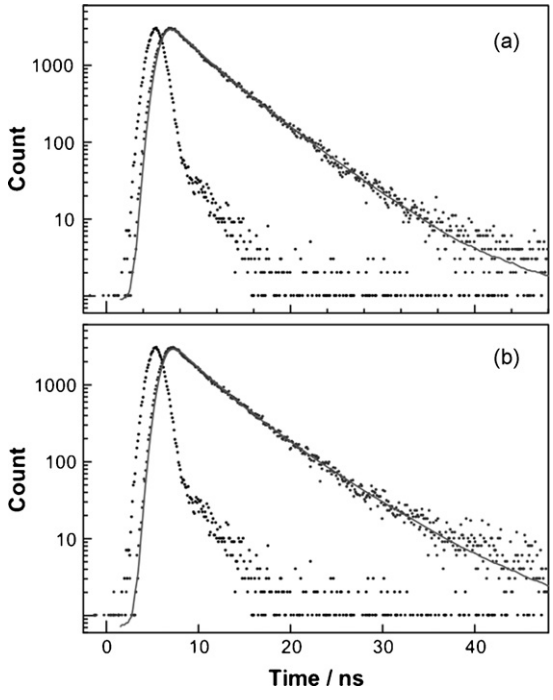

Fig. 3. Decay profiles for fluorescence of the aggregated $\mathbf{1}_n$ ((a) 1.5×10^{-2} M and (b) 2.0×10^{-2} M) in degassed ethanol monitored at 415 nm upon excitation of 345 nm light.

Table 2
Fluorescence decay lifetime (τ) and amplitude (A) of fluorescence from the aggregated $\mathbf{1}_n$

Concentration ($\times 10^{-2}$ M)	τ_1 (ns)	A_1 (%)	τ_2 (ns)	A_2 (%)	χ^2
1.5	2.1	27	4.8	73	1.04
2.0	2.9	50	5.8	50	1.28

The decay lifetime of the longer component was 5.8 ns, while decreasing its amplitude by 50%.

In contrast to a single component for other well-known J-aggregated systems [31,32], the present aggregated $\mathbf{1}_n$ exhibited two fluorescence decay components. However, our observations seem to be similar to the dye, which exhibited two or three different kinds of excitionic interactions by changing the content of dye adsorbed on solid thin films [33]. The excitation spectra with a vibronic shoulder are believed to be the exciton band resulting from the coexistence of a different kind of aggregate in a rigid environmental matrix [33]. Our observation of the two components of fluorescence decay is in accord with the two kinds of excitation bands (Table 1). This is also in agreement with the observation that the concentration dependence of the absorption spectra has no isosbetic point (Fig. 1).

Since the absorption and fluorescence spectral properties of the J-type aggregate depend on the geometry of the monomer unit in the aggregate, we performed an X-ray structural analysis on **1**. Upon recrystallization from ethanol, suitable crystals for X-ray diffraction studies were obtained, and the results are shown in Fig. 4. The interatomic distances of N2–C1 and N3–C3 are 1.392 and 1.380 Å, respectively, indicating that these interatomic bonds consist largely of σ bonding. Therefore, molecule **1** has a simple merocyanine skeleton. In the crystal packing, π–π stacking of molecule **1** aligned in parallel was observed by an inter-planar distance of 3.2 Å (Fig. 4b). Additionally, molecule **1** paired with itself by N2–H1···O1 (2.763 Å) self-

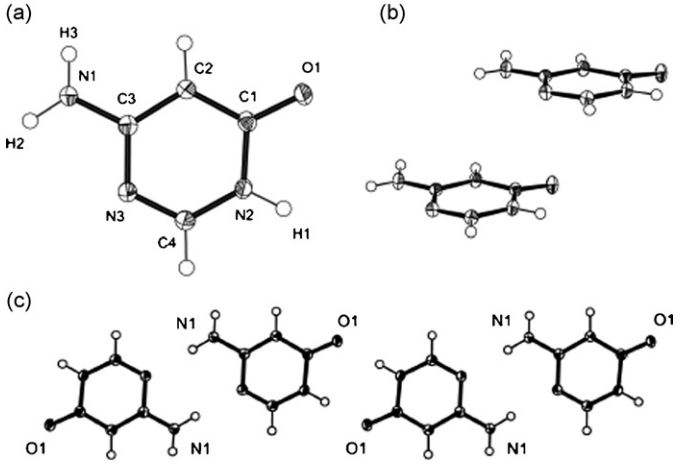

Fig. 4. (a) The ORTEP drawing of **1** together with the number scheme. The ellipsoids are drawn at the 50% probability. Selected inter-atomic distances (Å): C1–O1, 1.262(1); C1–C2, 1.396(1); C2–C3, 1.390(1); N1–C3, 1.339(1); N2–C1, 1.392(1); N3–C3, 1.380(1). Perspective view of (b) π–π stacking and (c) an infinite one-dimensional molecular arrangement by N2–H1···O1 (2.763 Å) and N1–H2···N3 (3.005 Å) hydrogen bonds.

complementary hydrogen bonding to form a centrosymmetric dimer. The dimer was further connected with other dimer pairs by the N1–H2···N3 (3.005 Å) hydrogen bonding, resulting in a 1D chain (Fig. 4c). It still remains to be determined whether the polarization axis of the band for the HOMO–LUMO transition led to an exciton coupling among the aggregated $\mathbf{1}_n$; however, it was found to be hardly assigned with the polarization direction by utilizing polarization spectrum. Nevertheless, the crystals of **1** obtained from ethanol were also found to show characteristic spectra (Fig. 7S). A diffuse reflection spectrum of **1** showed that the absorption tails off near 390 nm. Upon excitation with 340 nm light, the emission maximum appeared at a longer wavelength of 413 nm, which is shifted by 15 nm (912 cm^{-1}) as compared with that of the concentrated ethanol solution. By monitoring at 465 nm, the excitation maximum appears at 380 nm with a shoulder around 390 nm. These results clearly indicate that the J-type aggregates among the self-assembled **1** are present in the crystalline states.

4. Conclusions

The aggregated molecule **1** having the simple merocyanine skeleton showed an exciton coupling by formation of the J-type aggregate. Based on the optical studies and semi-empirical INDO/S CI calculations, the exciton band was formed by the red shift from the strongly allowed ππ* (HOMO–LUMO) state. The exciton state is also characterized by fluorescence emerging at longer wavelengths. The present J-type aggregate behavior of **1** is in sharp contrast to that of merocyanine derivatives, having a tendency to form the H-aggregate due to formation of the anti-parallel stacked dimer [11,14,15]. For molecule **1**, the aggregated structure was formed by parallel π–π stacking and hydrogen bonded chain arrangement with head-to-tail or oblique geometries in the crystalline state.

Acknowledgements

We wish to thank Dr. Tsutomu Ishi-i (Kurume National College of Technology) for use of the solid states fluorescence spectrometer, and Dr. Miki Hasegawa (Aoyama-Gakuin University) for many helpful discussions. This work was supported by a Grant-in-Aid for Scientific Research (no. 17510087) from the Ministry of Education, Culture, Sports, Science and Technology, Japan.

Appendix A. Supplementary data

Supplementary data associated with this article can be found, in the online version, at doi:10.1016/j.jphotochem.2007.07.019.

References

[1] V. Sundström, T. Pullerits, R. van Grondelle, J. Phys. Chem. B 103 (1999) 2327–2346.
[2] X. Hu, A. Damjanovíc, T. Ritz, K. Schulten, Proc. Natl. Acad. Sci. U.S.A. 95 (1998) 5935–5941.
[3] A.B. Doust, K.E. Wilk, P.M.G. Curmi, G.D. Scholes, J. Photochem. Photobiol. A: Chem. 184 (2006) 1–17.
[4] D. Möbius, Adv. Mater. 7 (1995) 437–444.
[5] A. Mishra, R.K. Behera, P.K. Behera, B.K. Mishra, G.B. Behera, Chem. Rev. 100 (2000) 1973–2011.
[6] O. Ohno, Y. Kaizu, H. Kobayashi, J. Chem. Phys. 99 (1993) 4128–4139.
[7] J.E. Maskasky, Langmuir 7 (1991) 407–421.
[8] G.J. Ashwell, G. Jefferies, D.G. Hamilton, D.E. Lynch, M.P.S. Roberts, G.S. Bahara, C.R. Brown, Nature 375 (1995) 385–388.
[9] F. Würthner, R. Wortmann, K. Meerholz, Chem. Phys. Chem. 3 (2000) 17–31.
[10] G.D. Scholes, G. Rumbles, Nat. Mater. 5 (2006) 683–696.
[11] F. Nüesch, M. Grätzel, Chem. Phys. 193 (1995) 1–17.
[12] F. Nüesch, J.E. Moser, V. Shklover, M. Grätzel, J. Am. Chem. Soc 118 (1996) 5420–5431.
[13] L. Lu, R.J. Lachicotte, T.L. Penner, J. Perlstein, D.G. Whitten, J. Am. Chem. Soc. 121 (1999) 8146–8156.
[14] F. Würthner, S. Yao, T. Debaerdemaeker, R. Wortmann, J. Am. Chem. Soc. 124 (2002) 9431–9447.
[15] S. Yao, U. Beginn, T. Gress, M. Lysetska, F. Würthner, J. Am. Chem. Soc. 126 (2004) 8336–8348.
[16] I. Baraldi, S. Ghelli, Z.A. Krasnaya, F. Momicchioli, A.S. Tatikolov, D. Vanossi, G. Ponterini, J. Photochem. Photobiol. A: Chem. 105 (1997) 297–305.
[17] J. Gao, C. Alhambra, J. Am. Chem. Soc. 119 (1997) 2962–2963.
[18] I. Baraldi, F. Momicchioli, G. Ponterini, A.S. Tatikolov, D. Vanossi, Phys. Chem. Chem. Phys. 5 (2003) 979–987.
[19] F. Meyers, S.R. Marder, B.M. Pierce, J.L. Brédas, J. Am. Chem. Soc. 116 (1994) 10703–10714.
[20] I.D.L. Albert, T.J. Marks, M.A. Ratner, J. Phys. Chem. 100 (1996) 9714–9725.
[21] P. Millié, F. Momicchioli, D. Vanossi, J. Phys. Chem. B 104 (2000) 9621–9629.
[22] D.J. Brown, J.S. Harper, J. Chem. Soc. (1961) 1298–1303.
[23] C.W. Whitehead, J.J. Traverso, J. Am. Chem. Soc. 82 (1960) 3971–3974.
[24] D.J. Brown, T. Teitei, Aust. J. Chem. 17 (1964) 567–572.
[25] J. Dąbrowski, K. Kamiénska-Trela, J. Am. Chem. Soc. 98 (1976) 2826–2834.
[26] C.A. Parker, T.A. Joyce, Trans. Faraday Soc. 62 (1966) 2785–2792.
[27] I. Tinoco Jr., J. Am. Chem. Soc. 82 (1960) 4785–4790.
[28] The parent merocyanine exhibits a positive solvatochromic property:
(a) B.F. Momicchioli, G. Ponterini, D. Vanossi, Chem. Phys. 238 (1998) 353–364;
(b) B.F. Momicchioli, G. Ponterini, D. Vanossi, Adv. Quantum Chem. 36 (1999) 121–150.
[29] M. Kasha, H.R. Rawls, M.A. El-Bayoumi, Pure Appl. Chem. 11 (1965) 371–392.
[30] E.E. Jelley, Nature 138 (1936) 1009–1010.
[31] The fluorescence life time of pseudoisocyanine J-aggregates:
(a) P.J. Reid, D.A. Higgins, P.F. Barbara, J. Phys. Chem. 100 (1996) 3892–3899;
(b) T. Tsubomura, O. Sakurai, M. Morita, J. Luminesc. 45 (1990) 263–265;
Thiacarbocyanine J-aggregates:
(c) M. Lindrum, A. Glismann, J. Moll, S. Daehne, Chem. Phys. 178 (1993) 232–423.
[32] I.G. Scheblyki, O.P. Varnavsky, W. Verbouwe, S. De Backer, M. Van der Auweraer, A.G. Vitukhnovsky, Chem. Phys. Lett. 282 (1998) 250–256.
[33] V. Martínez Martínez, F. López Arbeloa, J. Bañuelos Prieto, I. López Arbeloa, J. Phys. Chem. B 109 (2005) 7443–7450.